

# Finite compressibility in the low-doping region of the two-dimensional $t$ - $J$ model

Massimo Lugas, Leonardo Spanu, Federico Becca, and Sandro Sorella

*INFN-Democritos, National Simulation Center and International School for Advanced Studies (SISSA), I-34014 Trieste, Italy*

(Dated: May 11, 2018)

We revisit the important issue of charge fluctuations in the two-dimensional  $t$ - $J$  model by using an improved variational method based on a wave function that contains both the antiferromagnetic and the d-wave superconducting order parameters. In particular, we generalize the wave function introduced some time ago by J.P. Bouchaud, A. Georges, and C. Lhuillier [J. de Physique **49**, 553 (1988)] by considering also a *long-range* spin-spin Jastrow factor, in order to correctly reproduce the small- $q$  behavior of the spin fluctuations. We mainly focus our attention on the physically relevant region  $J/t \sim 0.4$  and find that, contrary to previous variational ansatz, this state is stable against phase separation for small hole doping. Moreover, by performing projection Monte Carlo methods based on the so-called fixed-node approach, we obtain a clear evidence that the  $t$ - $J$  model does not phase separate for  $J/t \lesssim 0.7$  and that the compressibility remains finite close to the antiferromagnetic insulating state.

PACS numbers:

## I. INTRODUCTION

The possible existence of charge and spin inhomogeneities and their relevance for the low-temperature physics of cuprates superconductors is a long-standing problem, not yet completely clarified.<sup>1</sup> In particular, the issue is twofold: On one hand, one is interested to understand the low-energy behavior of microscopic models and the possibility to have or not inhomogeneous phases in physically relevant regions; On the other hand, it is also important to clarify the possible relation between charge or spin inhomogeneities and the electronic pairing, which may lead to an high critical temperature for superconductivity.

The original interest in the role of these inhomogeneities dates back to the works by Emery and Kivelson<sup>2,3</sup> and raised when neutron scattering experiments<sup>4,5</sup> suggested the possible formation of conducting hole-rich regions separated from hole-poor ones with strong antiferromagnetic moments. Indeed, in most materials, the presence of a true phase separation (PS) instability is ruled out by the existence of the long-range Coulomb force that prevents the charge to accumulate in macroscopic regions,<sup>6</sup> only allowing the possibility to have a mesoscopic charge segregation, i.e., charge density waves (CDW) or the celebrated stripes. In the last decade, a great number of direct and indirect evidences for such charge segregation has been presented in different cuprate and nickelate materials, stimulating theoretical investigations in simple microscopic models.<sup>1</sup> Several authors addressed the possibility of the emergence of PS or CDW generating from the competition between the kinetic energy, that tends to delocalize the charge carriers, and various local interactions (like for instance the on-site Coulomb repulsion, the antiferromagnetic superexchange or the coupling with some local phonon), that instead tend to freeze the electrons.

Given the complexity of the strongly correlated problem, that contains different energy scales, it is very diffi-

cult to study its ground-state and low-energy properties. For instance, by considering mean-field approaches it is very easy to overestimate the tendency of charge segregation.<sup>7,8</sup> In this respect, a great advantage of the variational Monte Carlo technique is that it allows one to consider highly correlated wave functions, which are well beyond simple mean-field ansatz.<sup>9,10</sup> Then, it would be very important to compare the validity of the ansatz considered with exact ground-state properties on fairly large system sizes, since the variational approach may fail, especially for low-energy properties. This is possible only for bosonic non-frustrated models by means of quantum Monte Carlo projection techniques and for fermion systems the so-called sign problem prevents one to reach the exact zero-temperature properties in a stable way. Nevertheless, very well established and efficient approximate approaches are known for fermionic systems, that considerably improve the quality of a given variational guess. For instance, the so-called fixed node (FN) method (see below for a detailed description of the method on lattice models) allows one to obtain the lowest-energy state constrained to have the same signs of a given variational wave function. Therefore, the FN scheme provides a simple procedure to assess the stability of a particular variational wave function, its accuracy being related to the differences between its properties and the ones obtained with the improved FN state.

In this paper, we will revisit the problem of the PS instability in the  $t$ - $J$  model on the square lattice. This issue has been largely considered by several authors in the recent past.<sup>11,12,13,14,15,16,17</sup> Although, a great effort has been done, a general consensus for  $J/t \lesssim 0.6$  and small hole doping  $\delta$  is still lacking. The  $t$ - $J$  model is defined by:

$$\mathcal{H} = -t \sum_{\langle i,j \rangle \sigma} c_{i,\sigma}^\dagger c_{j,\sigma} + h.c. + J \sum_{\langle i,j \rangle} \left( \mathbf{S}_i \cdot \mathbf{S}_j - \frac{1}{4} n_i n_j \right), \quad (1)$$

where  $\langle \dots \rangle$  indicates the nearest-neighbor sites,  $c_{i,\sigma}^\dagger$

$(c_{i,\sigma})$  creates (destroys) an electron with spin  $\sigma$  on the site  $i$ ,  $\mathbf{S}_i = (S_i^x, S_i^y, S_i^z)$  is the spin operator,  $S_i^\alpha = \sum_{\sigma,\sigma'} c_{i,\sigma}^\dagger \tau_{\sigma,\sigma'}^\alpha c_{i,\sigma'}$ , being  $\tau^\alpha$  the Pauli matrices, and  $n_i = \sum_{\sigma} c_{i,\sigma}^\dagger c_{i,\sigma}$  is the density operator. We consider a square lattice with  $L$  sites and periodic boundary conditions rotated by 45 degrees such that  $L = 2l^2$ ,  $l$  being an odd integer, so that the non-interacting ground state is non-degenerate at half filling, thus reducing the finite-size effects. Finally,  $J$  is the antiferromagnetic exchange constant and  $t$  the amplitude for nearest-neighbor hopping. In the following we will take  $t = 1$ .

For very large  $J/t$ , at small hole doping, the ground state is phase separated between undoped regions, with long-range antiferromagnetic correlations, and conducting hole-rich regions. The simple explanation is based on the fact that the magnetic gain in accumulating the holes in a given region of space is much larger than the loss of the kinetic energy. Therefore, a phase separated state will have a lower energy than an homogeneous one. By decreasing  $J/t$ , the situation is much less clear, since the magnetic gain becomes comparable with the kinetic one. Emery, Kivelson, and Lin,<sup>3</sup> by using simple variational arguments, claimed that the ground state of the  $t-J$  model should phase separate for all values of the antiferromagnetic coupling and close to half filling. This claim was firstly confirmed by using a more sophisticated Monte Carlo technique<sup>12</sup>, but then disclaimed by other authors, using slightly different Monte Carlo approaches and series expansions.<sup>13,14,15,16</sup> In particular, two of us showed that, by filtering out the high-energy components of a projected BCS wave function, it was possible to obtain an homogeneous ground state for  $J/t \sim 0.4$ .<sup>15</sup> Later, this approach was questioned in Ref. 18, since it was noted that the ground state is still unstable against PS for very small hole doping, where our numerical approach had technical problems. In particular, it has been shown that Monte Carlo results could indicate an instability for  $\delta \lesssim 0.05$ . Moreover, it was disappointing that it was not possible to define a stable variational wave function and that an homogeneous state was obtained only after the filtering procedure. From all the calculations done by different numerical techniques, it is now clear that, in any case, the  $t-J$  model for  $J/t \sim 0.5$  is on the verge of charge instabilities, and both PS or CDW can be stabilized with small perturbations.<sup>19,20,21</sup>

A key issue that was absent in previous calculations and must be included in a correct description is the presence of antiferromagnetic correlations at low doping. Recently, by using a variational approach that contains both antiferromagnetism and d-wave pairing, Ivanov<sup>17</sup> suggested that the antiferromagnetic ordering could enhance the instability towards PS. However, in his approach, the presence of an antiferromagnetic order parameter in the fermionic determinant without the presence of a Jastrow term to take into account spin fluctuations implies a wrong behavior of the spin properties at small momenta, that in turn could also induce incorrect charge properties. In fact, by using a spin-wave approach

for the Heisenberg model, it has been shown<sup>22</sup> that an exceptionally accurate description of the ground state is obtained by applying a long-range spin Jastrow factor to the classically ordered state. In the corresponding variational wave function it is important that the Gaussian fluctuations induced by the Jastrow term are *orthogonal* to the direction of the order parameter, in order to reproduce correctly the low-energy excitations. A simple generalization of this wave function was used to study the Hubbard model at half filling and for low doping.<sup>23</sup> On the other hand, it is well known<sup>24,25,26</sup> that a projected BCS state with  $d_{x^2-y^2}$  symmetry and no antiferromagnetic order provides an accurate wave function for the low-doping region of the  $t-J$  model and remains rather accurate in energy even at zero doping, where a magnetically ordered ground state is well established in two dimensions. Therefore, in order to have an accurate variational ansatz to describe lightly doped correlated insulators, it seems natural to include both antiferromagnetic correlations and electronic pairing.<sup>27</sup>

Following these suggestions, we construct a very accurate variational wave function that describes an energetically stable homogeneous phase. Moreover, by considering the FN approach, we have a strong evidence in favor of an homogeneous ground state for  $J/t \lesssim 0.7$  for all the accessible hole doping.

The paper is organized as follow: in Sec. II we present the improved variational wave function and the FN method, in Sec. III we show our numerical results, and finally in Sec. IV we draw our conclusions.

## II. THE VARIATIONAL WAVE FUNCTION AND THE FN METHOD

In this section we describe the variational state and the generalized FN method that is used to filter out its high-energy components. Our variational ansatz is constructed by applying different projector operators to a mean-field state:

$$|\Psi_{VMC}\rangle = \mathcal{J}_s \mathcal{J}_d \mathcal{P}_N \mathcal{P}_G |\Psi_{MF}\rangle, \quad (2)$$

where  $\mathcal{P}_G$  is the Gutzwiller projector that forbids double occupied sites,  $\mathcal{P}_N$  is the projector onto the subspace with fixed number of  $N$  particles,  $\mathcal{J}_s$  is a spin Jastrow factor

$$\mathcal{J}_s = \exp \left( \frac{1}{2} \sum_{i,j} v_{ij} S_i^z S_j^z \right), \quad (3)$$

being  $v_{ij}$  variational parameters, and finally  $\mathcal{J}_d$  is a density Jastrow factor

$$\mathcal{J}_d = \exp \left( \frac{1}{2} \sum_{i,j} u_{ij} n_i n_j \right), \quad (4)$$

being  $u_{ij}$  other variational parameters. The above wave function can be efficiently sampled by standard variational Monte Carlo, by employing a random walk of a configuration  $|x\rangle$ , defined by the electron positions and their spin components along the  $z$  quantization axis. Indeed, in this case, both Jastrow terms are very simple to compute since they only represent classical weights acting on the configuration.

The main difference from previous approaches is the presence of the spin Jastrow factor and the choice of the mean-field state  $|\Psi_{MF}\rangle$ , that includes both superconducting and antiferromagnetic order parameters. Actually,  $|\Psi_{MF}\rangle$  is taken as the ground state of the mean-field Hamiltonian

$$\mathcal{H}_{MF} = \sum_{i,j,\sigma} t_{i,j} c_{i,\sigma}^\dagger c_{j,\sigma} + h.c. - \mu \sum_{i,\sigma} n_{i,\sigma} + \sum_{\langle i,j \rangle} \Delta_{i,j} (c_{i,\uparrow}^\dagger c_{j,\downarrow}^\dagger + c_{j,\uparrow}^\dagger c_{i,\downarrow}^\dagger + h.c.) + \mathcal{H}_{AF}, \quad (5)$$

where, in addition to the BCS pairing  $\Delta_{i,j}$  (with  $d$ -wave symmetry), we also consider a staggered magnetic field  $\Delta_{AF}$  in the  $x$ - $y$  plane:

$$\mathcal{H}_{AF} = \Delta_{AF} \sum_i (-1)^{R_i} (c_{i,\uparrow}^\dagger c_{i,\downarrow} + c_{i,\downarrow}^\dagger c_{i,\uparrow}), \quad (6)$$

where  $\Delta_{AF}$  is a variational parameter that, together with the chemical potential  $\mu$  and the next-nearest-neighbor hopping of Eq. (5), can be determined by minimizing the variational energy of  $\mathcal{H}$ . This kind of mean-field wave function was first introduced by Bouchaud, Georges, and Lhuillier<sup>28</sup> and then used to study  $\text{He}^3$  systems and small atoms and molecules.<sup>29,30</sup> Recently, it has been also used to study the  $t$ - $J$  model on the triangular lattice.<sup>31</sup> However, in these approaches the role of the long-range spin Jastrow factor was missed. We emphasize that, in the mean-field Hamiltonian (5), the magnetic order parameter is in the  $x$ - $y$  plane and not along the  $z$  direction like:

$$\mathcal{H}_{AF} = \Delta_{AF} \sum_i (-1)^{R_i} (c_{i,\uparrow}^\dagger c_{i,\uparrow} - c_{i,\downarrow}^\dagger c_{i,\downarrow}). \quad (7)$$

Indeed, as already mentioned in the introduction, only in the case of Eq. (6) the presence of the spin Jastrow factor (3) can introduce relevant fluctuations over the mean-field order parameter  $\Delta_{AF}$ , leading to an accurate description of the spin properties. By contrast, if the Jastrow potential is applied to the mean-field ansatz (7), it cannot induce correct spin fluctuations and it is not efficient in lowering the energy.

Finally, as already shown in Ref. 24, the presence of the density Jastrow factor helps to reproduce the charge correlations of the superconducting regime, giving rise to the correct Goldstone modes.

The mean-field Hamiltonian (5) is quadratic in the fermionic operators and can be easily diagonalized in real

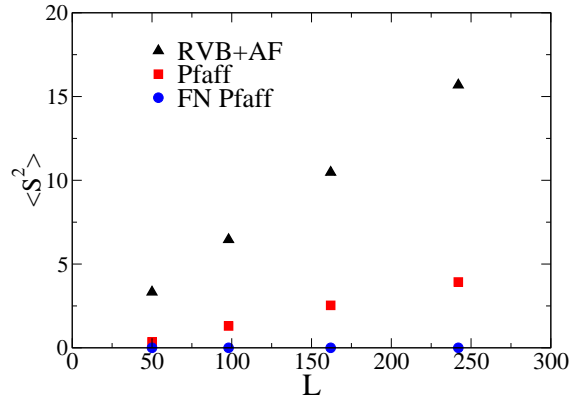


FIG. 1: Results for the total spin  $\langle S^2 \rangle$  at half filling as a function of the cluster size  $L$  for the wave function of Eq. (2) defined by the mean-field Hamiltonian (5) and the two possible orientations of the magnetic field, i.e., Eqs. (6), indicated by “Pfaff”, and (7), indicated by “RVB+AF”. The FN results for the former case are also shown.

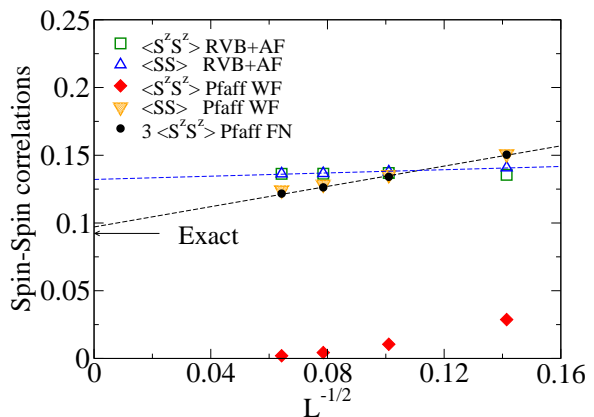


FIG. 2: Spin-spin correlations at the maximum distance at half filling for the wave functions of Fig. 1. The exact value in the thermodynamic limit is marked by the arrow.

space. Its ground state has the general form:

$$|\Psi_{MF}\rangle = \exp \left( \frac{1}{2} \sum_{i,j,\sigma_i,\sigma_j} f_{i,j}^{\sigma_i,\sigma_j} c_{i,\sigma_i}^\dagger c_{j,\sigma_j}^\dagger \right) |0\rangle, \quad (8)$$

the pairing function  $f_{ij}^{\sigma_i,\sigma_j}$  being an antisymmetric  $4L \times 4L$  matrix. Notice that in the case of the standard BCS Hamiltonian, with  $\Delta_{AF} = 0$  or even with  $\Delta_{AF}$  along  $z$ , we have that  $f_{i,j}^{\uparrow,\uparrow} = f_{i,j}^{\downarrow,\downarrow} = 0$ , while in presence of magnetic field in the  $x$ - $y$  plane the pairing function acquires non-zero contributions also in this triplet channel. The technical difficulty when dealing with such a state is that, given a generic configuration with definite  $z$ -component

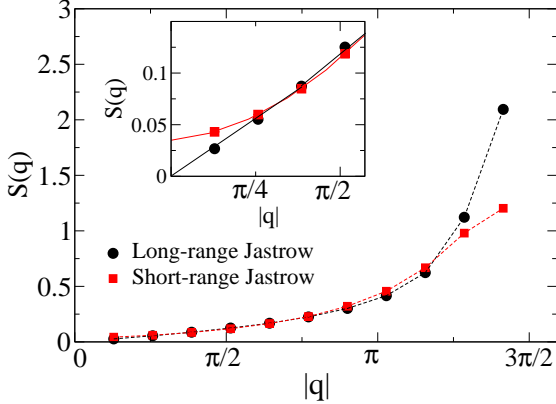


FIG. 3: Spin structure factor  $S(q)$  at half filling for the variational wave function of Eq. (2) defined by the mean-field Hamiltonian of Eqs. (5) and (6) with long-range and short-range (i.e., nearest-neighbor) Jastrow factors. Inset: Detail for small momenta.

of the spin  $|x\rangle = c_{i_1, \sigma_1}^\dagger \dots c_{i_N, \sigma_N}^\dagger |0\rangle$ , we have that:

$$\langle x | \Psi_{MF} \rangle = Pf[F], \quad (9)$$

where  $Pf[F]$  is the Pfaffian of the pairing function.<sup>32</sup> It should be noticed that, whenever  $f_{i,j}^{\uparrow, \uparrow} = f_{i,j}^{\downarrow, \downarrow} = 0$ , the usual form of  $\langle x | \Psi_{MF} \rangle$  written in terms of a determinant is recovered. The fact of dealing with Pfaffians makes the algorithm slower than the case of determinants, but the important point is that the algebra of Pfaffians still allows us to have a very efficient updating procedure in the Monte Carlo calculation. Then, by using the minimization technique described in Ref. 33, we are able to deal with a large number of variational parameters and in particular we can optimize all the independent coefficient  $v_{ij}$  and  $u_{ij}$ , beside the parameters contained in the mean-field Hamiltonian (5).

The variational accuracy of a given wave function can be assessed by the FN method that allows one to filter out the high-energy components of a given state and to find the best variational state with the same nodes of the starting one.<sup>34</sup> On the lattice, the FN method can be simply defined as follows: Starting from the original Hamiltonian  $\mathcal{H}$  we define an effective Hamiltonian by adding a perturbation  $O$ :

$$\mathcal{H}_{eff}^\gamma = \mathcal{H} + (1 + \gamma)O, \quad (10)$$

here we follow Ref. 35 and introduce the external parameter  $\gamma$ , the original FN approximation of Ref. 34 being recovered for  $\gamma = 0$ . The operator  $O$  is defined through its matrix elements and depends upon a given guiding function  $|\Psi\rangle$ , that is for instance the variational state itself, i.e.,  $|\Psi_{VMC}\rangle$ :

$$O_{x',x} = \begin{cases} -\mathcal{H}_{x',x} & \text{if } s_{x',x} = \Psi_{x'} \mathcal{H}_{x',x} \Psi_x > 0 \\ \sum_{y, s_{y,x} > 0} \mathcal{H}_{y,x} \frac{\Psi_y}{\Psi_x} & \text{for } x' = x, \end{cases}$$

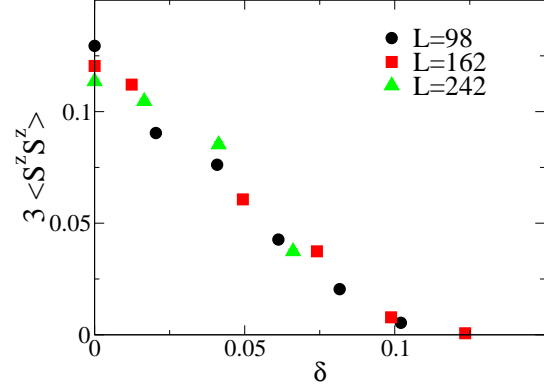


FIG. 4: FN results for the spin-spin correlations (along the  $z$  direction) at the maximum distance as a function of the doping for different sizes of the cluster.

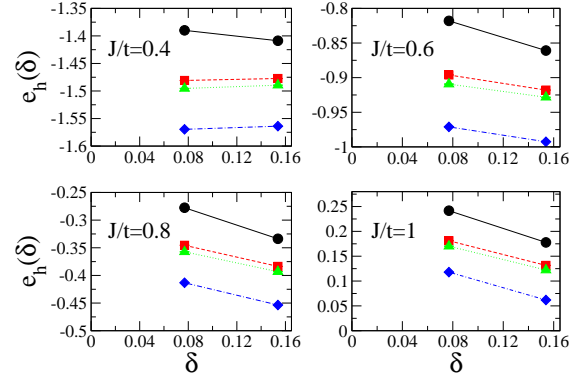


FIG. 5: Energy per hole  $e_h(\delta)$  as a function of the doping  $\delta$  for the 26-site cluster calculated by different approaches: The variational calculations for the Pfaffian wave function (circles), the FN approach of Eq. (11) (squares), and the expectation value of the Hamiltonian over the FN ground state given by Eq. (15) (triangles); the exact results are also shown (diamonds).

where  $\Psi_x = \langle x | \Psi \rangle$ . Notice that the above operator annihilates the guiding function, namely  $O|\Psi\rangle = 0$ . Therefore, whenever the guiding function is close to the exact ground state of  $\mathcal{H}$  the perturbation  $(1 + \gamma)O$  is expected to be small and the effective Hamiltonian becomes very close to the original one.

Let us review the properties of the FN Hamiltonian. Trivially, for  $\gamma = -1$ ,  $\mathcal{H}_{eff}^\gamma$  coincides with  $\mathcal{H}$ , as the perturbation vanishes. The most important property of this effective Hamiltonian is that for  $\gamma \geq 0$  its ground state  $|\Psi_0^\gamma\rangle$  can be efficiently computed by using the Green's function Monte Carlo technique,<sup>36,37</sup> that allows one to

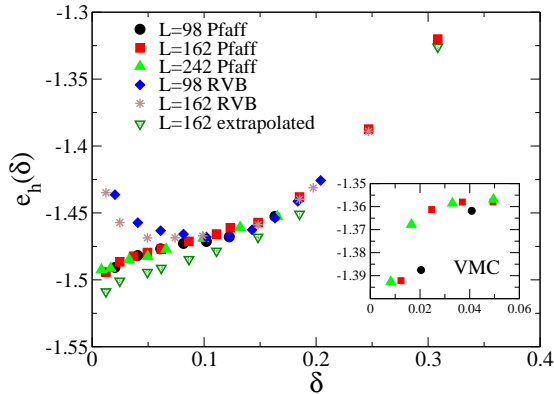


FIG. 6: Energy per hole  $e_h(\delta)$  as a function of the doping  $\delta$  for  $J/t = 0.4$  and different sizes. The results are obtained by using the FN approach described in the text. Two different states are used as guiding function: The simple non-magnetic state, denoted by “RVB” and the state with pairing, antiferromagnetism in the  $x-y$  plane, and the spin Jastrow factor, denoted by “Pfaff”. The expectation value of the Hamiltonian over the FN ground state are also shown for  $L = 162$  for the latter case. Inset: Variational energy per hole for the Pfaffian wave function.

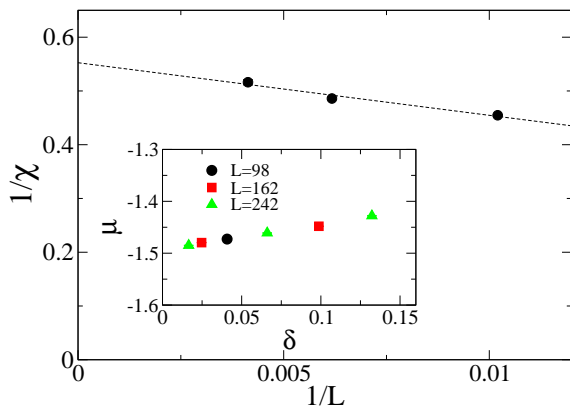


FIG. 7: The inverse compressibility of the half-filled Mott insulator for  $J/t = 0.4$  calculated by extracting the second derivative of the polynomial fit of the FN energy. Inset: The chemical potential, defined through the difference of ground-state energies, as a function of the doping for different sizes of the cluster.

sample the distribution  $\Pi_x \propto \langle x|\Psi\rangle\langle x|\Psi_0^\gamma\rangle$  by means of a statistical implementation of the power method:  $\Pi \propto \lim_{n \rightarrow \infty} G^n \Pi^0$ , where  $\Pi^0$  is a starting distribution and  $G_{x',x} = \Psi_{x'}(\Lambda \delta_{x',x} - \mathcal{H}_{eff,x',x}^\gamma)/\Psi_x$ , is the so-called Green’s function, defined with a large or even infinite<sup>38</sup> positive constant  $\Lambda$ ,  $\delta_{x',x}$  being the Kronecker symbol. The statistical method is very efficient for  $\gamma \geq 0$ , since in

this case all the matrix elements of  $G$  are non-negative and, therefore, it can represent a transition probability in configuration space, apart for a normalization factor  $b_x = \sum_{x'} G_{x',x}$ . In this case, it follows immediately that the asymptotic distribution  $\Pi$  is also positive and, therefore, we arrive at the important conclusion that for  $\gamma \geq 0$  the ground state of  $\mathcal{H}_{eff}^\gamma$  has the same signs of the chosen guiding function. Within the FN approximation, we have a direct access to the ground-state energy  $E_{FN}^\gamma$  of the effective Hamiltonian by sampling the so-called local energy  $e_L(x) = \langle x|\mathcal{H}|\Psi\rangle/\langle x|\Psi\rangle$  over the distribution  $\Pi_x$ . In the following, we will denote the standard FN energy for  $\gamma = 0$  simply by  $E_{FN}$ . It should be noted that, since  $O|\Psi\rangle = 0$ , we have that  $E_{FN}^\gamma$  is also the mixed average of the original Hamiltonian

$$E_{FN}^\gamma = \frac{\langle \Psi_0^\gamma | \mathcal{H}_{eff}^\gamma | \Psi_0^\gamma \rangle}{\langle \Psi_0^\gamma | \Psi_0^\gamma \rangle} = \frac{\langle \Psi | \mathcal{H} | \Psi_0^\gamma \rangle}{\langle \Psi | \Psi_0^\gamma \rangle}. \quad (11)$$

$E_{FN}^\gamma$  gives a rigorous upper bound of the exact ground-state energy  $E_0 = E_{FN}^{\gamma=0}$  since it is an increasing function of  $\gamma$  as the operator  $O$  is positive definite<sup>39</sup> and by the Hellman-Feynman theorem:

$$\frac{dE_{FN}^\gamma}{d\gamma} = \frac{d\langle \mathcal{H}_{eff}^\gamma \rangle}{d\gamma} = \langle \frac{d\mathcal{H}_{eff}^\gamma}{d\gamma} \rangle = \langle O \rangle \geq 0, \quad (12)$$

here  $\langle \dots \rangle$  indicates the expectation value over  $|\Psi_0^\gamma\rangle$ . This upper bound is also certainly below or equal to the variational energy of the guiding function  $E = \langle \Psi | \mathcal{H} | \Psi \rangle / \langle \Psi | \Psi \rangle$ , since from  $O|\Psi\rangle = 0$  it follows that  $E$  is also the expectation value of the FN Hamiltonian over  $|\Psi\rangle$ , namely  $E = \langle \Psi | \mathcal{H}_{eff}^\gamma | \Psi \rangle / \langle \Psi | \Psi \rangle$ .

One of the advantages of having introduced the parameter  $\gamma$  is that it is possible to extract the expectation value of the original Hamiltonian  $\mathcal{H}$  over the FN state  $|\Psi_0^\gamma\rangle$ . Indeed, by applying Eq. (12), we have that:

$$\begin{aligned} E_{\Psi_0}^\gamma &= \langle \mathcal{H} \rangle = \langle \mathcal{H}_{eff}^\gamma \rangle - (1 + \gamma) \frac{d\langle \mathcal{H}_{eff}^\gamma \rangle}{d\gamma} \\ &= E_{FN}^\gamma - (1 + \gamma) \frac{dE_{FN}^\gamma}{d\gamma}, \end{aligned} \quad (13)$$

and therefore, by doing simulations for different values of  $\gamma$  to calculate numerically the derivative, it is possible to evaluate the expectation value of  $\mathcal{H}$  over the ground state of the FN Hamiltonian. Moreover, by using the definition (13) and the fact that  $E_{FN}^\gamma$  is a convex function,<sup>35</sup> it turns out that:

$$\frac{dE_{\Psi_0}^\gamma}{d\gamma} = -(1 + \gamma) \frac{d^2 E_{FN}^\gamma}{d\gamma^2} > 0, \quad (14)$$

namely  $E_{\Psi_0}^\gamma$  is monotonically increasing with  $\gamma$ . A practical estimate of  $E_{\Psi_0}^{\gamma=0}$ , the best variational energy that can be obtained within a stable statistical method, can be worked out by performing two calculations for  $\gamma = 0$  and  $\gamma = \tilde{\gamma} > 0$  via:

$$\tilde{E}_{\Psi_0}^{\gamma=0} = E_{FN} - \frac{1}{\tilde{\gamma}} (E_{FN}^{\tilde{\gamma}} - E_{FN}), \quad (15)$$

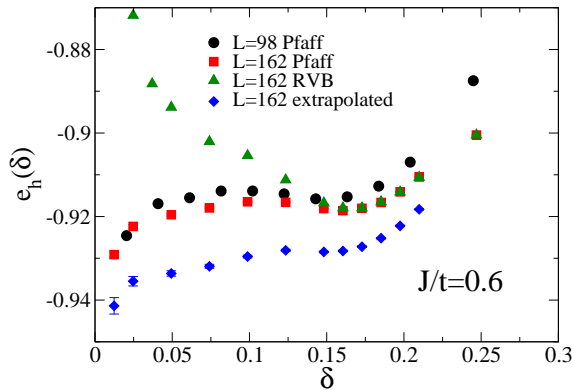


FIG. 8: The same as in Fig. 6 for  $J/t = 0.6$ .

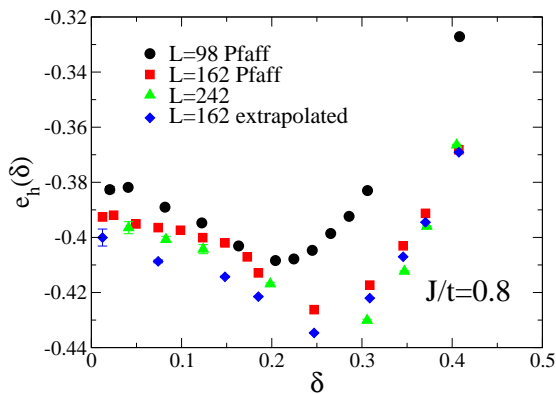


FIG. 9: The same as in Fig. 6 for  $J/t = 0.8$ .

$\tilde{E}_{\Psi_0}^{\gamma=0}$  certainly improves the standard FN upper bound of the energy and still  $\tilde{E}_{\Psi_0}^{\gamma=0} \geq E_{\Psi_0}^{\gamma=0}$ . This latter inequality follows from the convexity of  $E_{FN}^{\gamma}$ , implying that its first derivative at  $\gamma = 0$  is certainly larger or equal than the corresponding finite difference estimate. In order to obtain a compromise between having small enough statistical errors and a reasonable energy gain with respect to the mixed average of Eq. (11), we have computed  $\tilde{E}_{\Psi_0}^{\gamma=0}$  using  $\tilde{\gamma} = 1$ .

In order to show the accuracy of the wave function (2) and the FN method, we report in Table I and II the energies for 2 and 4 holes in 26 sites compared with the exact diagonalization data; in the same table we also show the results obtained from the wave function without the antiferromagnetic order parameter. Finally, we report the values of the extrapolated energies  $\tilde{E}_{\Psi_0}^{\gamma=0}$  given by Eq. (15). The inclusion of the magnetic field and the spin Jastrow factor strongly improve the energies with respect to the non-magnetic wave function.

In particular, at half filling the FN is *exact* (within the error-bars), i.e.,  $E_{FN}/L = -1.184450(2)$  (in unit of  $J = 1$ ), whereas the variational energy is already very good  $E_{VMC}/L = -1.18213(1)$ . On the other hand, although the signs of the non-magnetic wave function are correct (with the choice of  $t_{i,j}$  and  $\Delta_{i,j}$  connecting opposite sublattices and  $\mu = 0$ ), the non-magnetic wave function vanishes on many relevant configurations. This implies that, due to the importance sampling procedure described before, such configurations are never visited by the Markov process, leading to  $E_{FN}/L = -1.1833(3)$ , despite the fact that the variational energy is not so poor  $E_{VMC}/L = -1.15334(1)$ . We also notice that in this case the FN is highly unstable and many walkers are needed to stabilize its convergence.

It is important to stress that the concomitant presence of the magnetic order parameter  $\Delta_{AF}$ , that breaks the  $SU(2)$  spin symmetry of the electronic part, and the spin Jastrow factor of Eq. (3), that also breaks the spin symmetry, gives rise to an almost symmetric state, even for large sizes. This can be verified by calculating the total spin  $S^2$ : In Fig. 1 we report the results for the two wave functions with magnetic order in the  $x-y$  plane and along the  $z$  direction, usually considered to describe the lightly doped region.<sup>17,40</sup> In the same figure, we also report the FN value of  $S^2$  (by using the former state as the guiding function) in order to show that a totally symmetric state is eventually recovered.

By a direct calculation of the spin-spin correlations at the maximum distance, we obtain that also the value of the magnetization at half filling is in a very good agreement with the exact result,<sup>37,41</sup> see Fig. 2. It should be noted that the variational wave function with the magnetization in the  $x-y$  plane and the spin Jastrow factor has very accurate isotropic spin-spin correlations, though in the  $z$  direction they decay to zero in the thermodynamic limit. By performing the FN approach (with  $\gamma = 0$ ), a finite value for the correlations along  $z$  is recovered. By contrast, when the magnetization is directed along  $z$  in the variational ansatz, the spin correlations are almost Ising-like in the same direction and lead to overestimate the thermodynamic value of the magnetization, namely  $m \sim 0.37$ , see Fig. 2.

Finally, we want to stress that the long-range tail of the spin Jastrow factor, obtained by minimizing the energy and leading to  $v_q \sim 1/|q|$  for small  $|q|$  ( $v_q$  being the Fourier transform of  $v_{ij}$ ), is necessary to correctly reproduce the small- $q$  behavior of the spin-structure factor

$$S(q) = \frac{1}{L} \sum_{l,m} e^{iq(R_l - R_m)} S_l^z S_m^z. \quad (16)$$

Indeed, as it is clear from Fig. 3, only with a long-range spin Jastrow factor, it is possible to obtain  $S(q) \sim |q|$  for small momenta and, therefore, a gapless spin spectrum. By contrast, with a short-range spin Jastrow term (for instance with a nearest-neighbor term),  $S(q) \sim \text{const}$ , for small  $q$ , that is clearly not correct.

TABLE I: Ground state energy for 2 holes on 26 sites and different values of  $J/t$ . Two wave function with and without  $\Delta_{AF}$  are indicated with ‘‘Pfaff’’ and ‘‘RVB’’, respectively. The variational results are indicated by VMC and the fixed-node ones by FN. In the last two columns we report the extrapolated value of Eq. (15) with the Pfaffian wave function and exact results by Lanczos method, respectively.

$J/t$	$E_{VMC}^{RVB}/L$	$E_{FN}^{RVB}/L$	$E_{VMC}^{Pfaff}/L$	$E_{FN}^{Pfaff}/L$	$\tilde{E}_{\Psi_0}^{\gamma=0}/L$	$E_{ex}/L$
0.3	-0.48334(1)	-0.49256(1)	-0.48476(1)	-0.49325(1)	-0.49445(2)	-0.50097
0.4	-0.57664(1)	-0.58625(1)	-0.57978(1)	-0.58770(1)	-0.58881(2)	-0.59452
0.5	-0.67045(1)	-0.68091(1)	-0.67568(1)	-0.68327(1)	-0.68434(3)	-0.68945
0.6	-0.76463(1)	-0.77645(1)	-0.77228(1)	-0.77960(1)	-0.78062(3)	-0.78537
0.8	-0.95410(1)	-0.96920(1)	-0.96706(1)	-0.97414(1)	-0.97505(3)	-0.97935
1.0	-1.14483(1)	-1.16385(1)	-1.16352(1)	-1.17052(1)	-1.17136(2)	-1.17538

TABLE II: The same as in Table I but for 4 holes on 26 sites.

$J/t$	$E_{VMC}^{RVB}/L$	$E_{FN}^{RVB}/L$	$E_{VMC}^{Pfaff}/L$	$E_{FN}^{Pfaff}/L$	$\tilde{E}_{\Psi_0}^{\gamma=0}/L$	$E_{ex}/L$
0.3	-0.61372(1)	-0.62752(1)	-0.61478(1)	-0.62754(1)	-0.62958(3)	-0.64262
0.4	-0.68894(1)	-0.70101(1)	-0.68946(1)	-0.70106(1)	-0.70292(2)	-0.71437
0.5	-0.76461(1)	-0.77571(1)	-0.76512(1)	-0.77595(1)	-0.77770(4)	-0.78812
0.6	-0.84065(1)	-0.85132(1)	-0.84170(1)	-0.85189(1)	-0.85348(3)	-0.86337
0.8	-0.99361(1)	-1.00476(1)	-0.99709(1)	-1.00659(1)	-1.00806(2)	-1.01733
1.0	-1.14760(1)	-1.16072(1)	-1.15479(1)	-1.16422(1)	-1.16566(3)	-1.17493

### III. RESULTS

Before considering the PS instability, we show in Fig. 4 the results for the spin-spin correlations at the maximum distance as a function of the doping. We have that the magnetic order survives up to  $\delta \sim 0.1$ , in agreement with previous calculations<sup>17,42</sup> and showing the importance to include the magnetic parameter into the variational wave function. Unfortunately, a precise size scaling analysis is not possible at finite hole concentration, since only discrete values of the doping are achievable and very rarely they are compatible from cluster to cluster.

Let us move to the central issue of this work. In order to detect a possible PS instability, it is convenient to follow the criterion given in Ref. 3 and consider the energy per hole:

$$e_h(\delta) = \frac{e(\delta) - e(0)}{\delta}, \quad (17)$$

where  $e(\delta)$  is the energy per site at hole doping  $\delta$  and  $e(0)$  is its value at half filling. For a stable system,  $e_h(\delta)$  must be a monotonically increasing function of  $\delta$ , since in this case the energy is a convex function of the doping and  $e_h(\delta)$  represents the chord joining half filling and the doping  $\delta$ . On the other hand, the PS instability is marked by a minimum at a given  $\delta_c$  on finite clusters, and a flat behavior up to  $\delta_c$  in the thermodynamic limit where the Maxwell construction is implied.

Firstly, Fig. 5 shows the results of  $e_h(\delta)$  for different ratios  $J/t$  on the 26-site cluster, where the exact data are available by the Lanczos method. Although these data are already contained in tables I and II, their graphical representation better shows our accuracy to estimate the slope of the energy per hole. In particular, we stress the fact that, even though already the variational results of

the wave function (2) are very accurate, there is a strong improvement by considering the FN approach, both in the mixed average of Eq. (11) and in the extrapolation of Eq. (15), for which a perfect estimation of the slope is obtained.

Then we can move to large cluster to extract the thermodynamic properties. We report in Fig. 6 the results of the energy per hole for  $J/t = 0.4$ . For comparison, the FN calculations for  $\gamma = 0$  are performed by using two different guiding functions, including or not the antiferromagnetic order parameter and the spin Jastrow factor. At large doping the results are independent on the choice of the guiding state, clearly indicating that the antiferromagnetism is not essential. However, by decreasing the hole concentration, the inclusion of the antiferromagnetic order becomes crucial for the stabilization of the homogeneous phase, whereas the simple projected BCS state is eventually unstable at small doping. This latter outcome actually is in agreement with our previous calculations<sup>15</sup> and confirms what has been noticed by Hellberg and Manousakis<sup>18</sup> and interpreted as an evidence for PS close to the insulating limit. By contrast, our present FN results, based on the wave function with antiferromagnetic fluctuations, strongly improve the accuracy of previous calculations for small doping and point towards the stability of the homogeneous phase for all hole concentrations. Quite impressively, the energies are very accurate on the whole doping regime analyzed and there is not a qualitative difference if one considers the expectation value of the Hamiltonian (15), see Fig 6. These results indicate that the ground state is stable for all the hole concentrations, namely down to  $\delta \sim 0.01$  (i.e., two holes on 242 sites), strongly improving our previous estimate of the phase diagram. Remarkably, also the variational wave function is stable for such value of

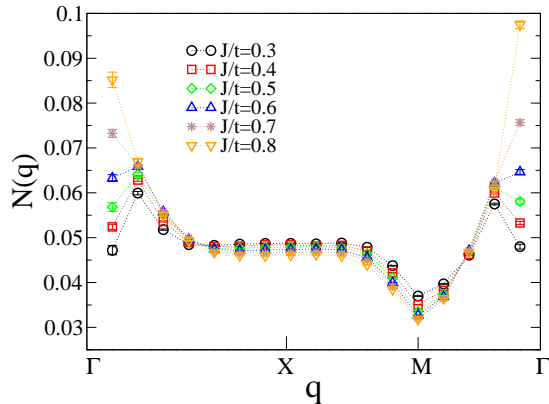


FIG. 10: FN results for the density correlation function for 8 holes on 162 sites and different values of  $J/t$ . The high-symmetry points are marked as  $\Gamma = (0, 0)$ ,  $X = (\pi, \pi)$ , and  $M = (\pi, 0)$ .

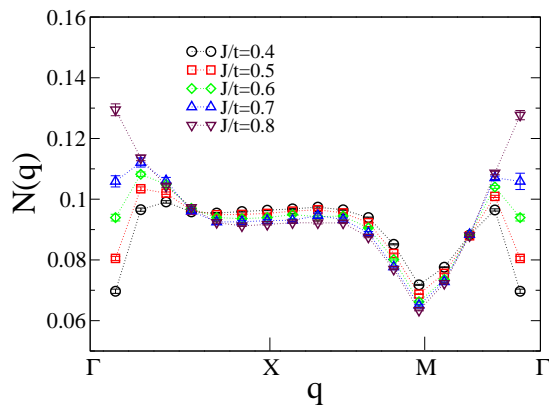


FIG. 11: The same as in Fig. 10 but for 16 holes on 162 sites.

the super-exchange interaction and small hole concentrations, see the inset of Fig. 6. To our knowledge, this is the first successful attempt to obtain a variational state which is clearly stable towards the formation of regions with segregated holes, when approaching the Mott insulating regime.

From the energy calculation it is straightforward to estimate the compressibility  $\chi$  for  $\delta \rightarrow 0$ :

$$\chi^{-1} = \frac{\partial^2 e(\delta)}{\partial \delta^2}. \quad (18)$$

Recently, Imada and coworkers,<sup>43,44</sup> by using hyperscaling arguments and numerical simulations on the Hubbard model, proposed that the compressibility must diverge when the insulating phase is approached by decreasing the doping concentration. Their arguments imply that  $e(\delta) \sim \delta^3$  for small doping, as in the one-

dimensional case, where the charge properties can be simply understood by considering spinless fermions. Instead, within our FN approach, we find that the compressibility stays finite up to half filling. Indeed, for  $J/t = 0.4$  and in general for the stable magnetic phase, the variational calculation provides a finite compressibility that is further decreased by the more accurate FN approximation. It should be noticed that a much larger compressibility, or even an infinite one, could be worked out when considering only small size calculations, like the ones used in Ref. 43 to obtain  $\chi \sim |\mu - \mu_c|^{-1/2} \sim \delta^{-1}$  (where  $\mu$  is the chemical potential and  $\mu_c$  is nothing but the charge gap at half filling): In this case, it is possible to underestimate the slope of the energy at small doping and, therefore, also to overestimate the value of  $\chi$ . Instead, from our large cluster calculations, we have a clear evidence that the chemical potential is linear with the doping close to half filling or, equivalently, that  $e(\delta) \sim \delta^2$ , implying a finite compressibility when  $\delta \rightarrow 0$ , see Fig. 7. Our calculations are rather robust and do not depend upon the number of holes considered and a very accurate polynomial fit of the energy turns out to be very stable. We argue that the infinite compressibility scenario proposed by Imada and coworkers could be correct when the antiferromagnetism does not play an important role and the undoped system is a spin liquid with no magnetic order. This is also supported by dynamical mean-field theory calculations by Kotliar and coworkers<sup>45</sup> on the Hubbard model, where the mean-field solution without an antiferromagnetic order parameter leads to a diverging compressibility close to the Mott regime.

By increasing the antiferromagnetic super-exchange, we come closer to the PS region. Indeed, for  $J/t = 0.6$  we obtain that the energy per hole  $e_h(\delta)$  shows a slightly non-monotonic behavior with a minimum for  $\delta_c \sim 0.17$ , when considering the FN energies. This minimum disappears by performing the extrapolation of Eq. (15) to estimate the expectation value of the  $t-J$  Hamiltonian over the FN ground state, see Fig. 8. This fact would indicate that, for this value of  $J/t$ , the FN Hamiltonian (10) has a higher tendency towards PS than the original  $t-J$  model. In this case, the mixed average of Eq. (11) is slightly biased, and this bias can be eliminated by considering the actual expectation value of the  $t-J$  Hamiltonian over the FN ground state. In doing this, we approach the exact result (by improving the energy) and a homogeneous phase, with a monotonically increasing energy per hole, is obtained. Within this more accurate scheme, we substantially improve our previous results that were based on the mixed average of the FN approximation and that indicated a rather high critical doping.<sup>15</sup> Unfortunately, within our numerical approach, it is very difficult to study the possible formation of hole droplets close to the PS instability, as suggested by Poilblanc.<sup>46</sup> Indeed, this would require a very delicate size scaling of the binding energy of few holes, which is beyond our present possibilities.

By further increasing the super-exchange coupling, we



## IV. CONCLUSION

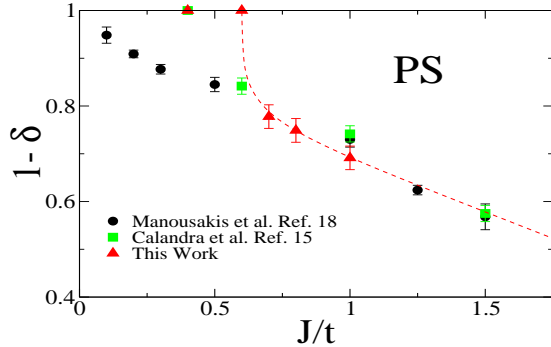


FIG. 12: Boundary for the phase separation (PS) instability. The results of previous works are also shown for comparison. The line is a guide to the eye.

eventually enter into the PS region: For  $J/t = 0.8$ , the energy per hole has a rather deep minimum at finite doping and also the expectation value (15) clearly indicates a non-monotonic behavior, see Fig. 9.

Finally, it is important to stress that very similar results can be also obtained by considering the density-density correlation function

$$N(q) = \frac{1}{L} \sum_{l,m} e^{iq(R_l - R_m)} n_l n_m. \quad (19)$$

In this case, since  $N(q)$  is a diagonal operator in the configuration space, it is easy to compute its average value over the FN ground state by using the so-called forward-walking technique.<sup>37</sup> This quantity is therefore free from possible bias coming from mixed averages. The PS instability is signaled by the divergence at small momenta of  $N(q)$ . In our previous paper,<sup>15</sup> we reported the calculations of this quantity, showing the presence of a finite- $q$  peak, linearly depending upon the doping, close to the PS instability. Here, thanks to the accuracy of the guiding function and the progress in stabilizing the statistical implementation of the FN technique, we are able to present much more accurate results that confirm the previous ones. Indeed, the existence of this peak is due to the closeness of the PS: Figs. 10 and 11 show the evolution of  $N(q)$  by increasing  $J/t$  for two values of the doping, near the insulating regime. In particular, we obtain the evidence for a stable homogeneous phase for  $J/t \sim 0.4$ , confirming the indications given by the analysis based upon the energy per hole. Then also the progressive development of a huge peak around  $q = (0, 0)$  for  $J/t \sim 0.7$  is in good agreement with the energy calculations. All together, these results allow us to draw our final phase diagram of Fig. 12, where we report, for comparison, also some of the previous estimations for the PS boundaries.

We have revisited the problem of the PS instability in the  $t$ - $J$  model. By generalizing the Pfaffian wave function introduced some time ago,<sup>28</sup> we have defined a very accurate variational state that, for the first one to our knowledge, is stable against PS at low doping. In particular, we have shown the necessity to consider both an antiferromagnetic order parameter (in the fermionic determinant) and a spin Jastrow factor, to mimic the spin fluctuations. In this way all the low-energy properties of the exact ground state are correctly reproduced. Then, by using a more sophisticated Monte Carlo technique that can filter out the high-energy components of a given trial wave function, we can obtain the ground state of an effective Hamiltonian and, at the same time, assess the stability our initial guess. So, we have shown that for  $J/t = 0.4$ , the ground state does not phase separate at any hole doping down to  $\delta \sim 0.01$ , giving a serious improvement on the possible PS boundaries at small  $J/t$ . Remarkably, the analysis based on the energy per hole is also corroborated by the calculation of the static density-density correlations. The phase separation, in the low doping region, appears at a critical antiferromagnetic coupling slightly larger than the value given in Ref. 15, namely here we find  $J_c/t \sim 0.7$ . Although future improvements in the Monte Carlo technique or in the accuracy of the variational wave function may lead to an higher coupling, it looks unlikely to reach the critical point recently obtained by high-temperature expansion,<sup>11,16</sup> i.e.,  $J_c/t \sim 1.2$ . In fact, as shown in Fig. 5, our present accuracy in the energy per hole is about  $0.05t$  and its slope is almost correct. This holds rather independently of  $J/t$  and system sizes, at least for the clusters where exact results are available. For  $J/t = 0.8$  (see Fig. 9), the minimum of the energy per hole implies an energy gain for the inhomogeneous phase of about  $0.05t$  per hole, i.e., comparable with our maximum possible error estimated before. Thus we expect that  $J_c/t$  cannot be much larger than 0.8 even for a numerically exact method.

Moreover, we have obtained that, in contrast with what was found in the Hubbard model, the compressibility stays finite by approaching the Mott insulator. A simple explanation of a finite compressibility in two dimensions is obtained by assuming that the holes form hole pockets around the nodal points [i.e.,  $q = (\pm\pi/2, \pm\pi/2)$ ] and behave as spinless fermions, implying that  $e(\delta) \simeq \delta^{1+2/D}$ , where  $D$  is the spatial dimension. In this simple scenario the compressibility is divergent only in one dimension, whereas it is finite in two dimensions, and should approach zero in three dimensions, leading to a more conventional metal-insulator transition.

The stability against phase separation of a wave function with explicit antiferromagnetism and d-wave superconducting order parameter provides new insights for understanding the phase diagram of the high-temperature superconductors. Remarkably, in the clean system, pos-

sibly idealized by the  $t$ - $J$  model, the antiferromagnetism and the d-wave order parameter should not exclude each other, at least at the variational level, and actually cooperate to decrease the energy and lead to a stable ho-

mogeneous phase.

This research has been supported by PRIN-COFIN 2005 and CNR-INFM.

- 
- <sup>1</sup> For a recent review, see for instance, S.A. Kivelson, I.P. Bindloss, E. Fradkin, V. Oganesyan, J.M. Tranquada, A. Kapitulnik, and C. Howald, *Rev. Mod. Phys.* **75**, 1201 (2003). See also, E.W. Carlson, V.J. Emery, S.A. Kivelson, and D. Orgad, *cond-mat* 0206217.
- <sup>2</sup> V.J. Emery and S.A. Kivelson, *Physica C* **209**, 597 (1993).
- <sup>3</sup> V.J. Emery, S.A. Kivelson, and H.Q. Lin, *Phys. Rev. Lett.* **64**, 475 (1990).
- <sup>4</sup> J.M. Tranquada, B.J. Sternlieb, J.D. Axe, Y. Nakamura, and S. Uchida, *Nature (London)* **375**, 561 (1995).
- <sup>5</sup> J.M. Tranquada, J.D. Axe, N. Ichikawa, A.R. Moodenbaugh, Y. Nakamura, and S. Uchida, *Phys. Rev. Lett.* **78**, 338 (1997).
- <sup>6</sup> To our knowledge, the only cuprate superconductor showing PS is  $\text{La}_2\text{CuO}_{4+\delta}$ , due to the presence of mobile apical Oxygens that can screen the Coulomb potential of the mobile charges in the  $\text{CuO}_2$  plane. See for instance, J.D. Jorgensen, B. Dabrowski, S. Pei, D.G. Hinks, L. Soderholm, B. Morosin, J.E. Schirber, E.L. Venturini, and D.S. Ginley, *Phys. Rev. B* **38**, 11337 (1988).
- <sup>7</sup> D. Poilblanc and T.M. Rice, *Phys. Rev. B* **39**, 9749 (1989).
- <sup>8</sup> H.J. Schultz, *Phys. Rev. Lett.* **64**, 1445 (1990).
- <sup>9</sup> C. Gros, *Phys. Rev. B* **38**, 931 (1988).
- <sup>10</sup> H. Yokoyama and H. Shiba, *J. Phys. Soc. Jpn.* **56** 1490 (1987); **56**, 3582 (1987); **56**, 1490 (1987).
- <sup>11</sup> W.O. Putikka, M.U. Luchini, and T.M. Rice, *Phys. Rev. Lett.* **68**, 538 (1992).
- <sup>12</sup> C.S. Hellberg and E. Manousakis, *Phys. Rev. Lett.* **78**, 4609 (1997).
- <sup>13</sup> M. Kohno, *Phys. Rev. B* **55**, 1435 (1997).
- <sup>14</sup> C.T. Shih, Y.C. Chen, and T.K. Lee, *Phys. Rev. B* **57**, 627 (1998).
- <sup>15</sup> M. Calandra, F. Becca, and S. Sorella, *Phys. Rev. Lett.* **81**, 5185 (1998).
- <sup>16</sup> W.O. Putikka and M.U. Luchini, *Phys. Rev. B* **62**, 1684 (2000).
- <sup>17</sup> D.A. Ivanov, *Phys. Rev. B* **70**, 104503 (2004).
- <sup>18</sup> C.S. Hellberg and E. Manousakis, *Phys. Rev. B* **61**, 11787 (2000).
- <sup>19</sup> S.R. White and D.J. Scalapino, *Phys. Rev. Lett.* **80**, 1272 (1998).
- <sup>20</sup> S.R. White and D.J. Scalapino, *Phys. Rev. B* **61**, 6320 (2000).
- <sup>21</sup> F. Becca, L. Capriotti, and S. Sorella, *Phys. Rev. Lett.* **87**, 167005 (2001).
- <sup>22</sup> F. Franjic and S. Sorella, *Prog. Theor. Phys.* **97**, 399 (1997).
- <sup>23</sup> F. Becca, M. Capone, and S. Sorella, *Phys. Rev. B* **62**, 12700 (2000).
- <sup>24</sup> S. Sorella, G.B. Martins, F. Becca, C. Gazza, L. Capriotti, A. Parola, and E. Dagotto, *Phys. Rev. Lett.* **88**, 117002 (2002).
- <sup>25</sup> A. Paramekanti, M. Randeria, and N. Trivedi, *Phys. Rev. Lett.* **87**, 217002 (2001).
- <sup>26</sup> D.A. Ivanov, P.A. Lee, and X.-G. Wen, *Phys. Rev. Lett.* **84**, 3958 (2000).
- <sup>27</sup> E. Plekhanov, F. Becca, and S. Sorella, *Phys. Rev. B* **71**, 064511 (2005).
- <sup>28</sup> J.P. Bouchaud, A. Georges, and C. Lhuillier, *J. Phys. (Paris)* **49**, 553 (1988).
- <sup>29</sup> J. Carlson, S.-Y. Chang, V.R. Pandharipande, and K.E. Schmidt, *Phys. Rev. Lett.* **91**, 050401 (2003).
- <sup>30</sup> M. Bajdich, L. Mitas, G. Drobný, L.K. Wagner, and K.E. Schmidt, *Phys. Rev. Lett.* **96**, 130201 (2006).
- <sup>31</sup> C. Weber, A. Lauchli, F. Mila, and T. Giamarchi, *Phys. Rev. B* **73**, 014519 (2006).
- <sup>32</sup> In general, the Pfaffian of a  $2n \times 2n$  antisymmetric matrix  $\chi$  is equal to the antisymmetric product of its matrix elements, i.e.,  $Pf[\chi] = \mathcal{A}\{\chi_{1,2}\chi_{3,4}\dots\chi_{2n-1,2n}\}$ , with the constraint that each term  $\chi_{i_1,j_1}\chi_{i_2,j_2}\dots\chi_{i_n,j_n}$  has  $i_k < j_k$  and  $i_1 < i_2 < \dots < i_n$ .
- <sup>33</sup> S. Sorella, *Phys. Rev. B* **71**, 241103 (2005).
- <sup>34</sup> D.F.B. ten Haaf, H.J.M. van Bommel, J.M.J. van Leeuwen, W. van Saarloos, and D.M. Ceperley, *Phys. Rev. B* **51**, 13039 (1995).
- <sup>35</sup> S. Sorella, *cond-mat/0201388*.
- <sup>36</sup> N. Trivedi and D. Ceperley, *Phys. Rev. B* **41**, 4552 (1990).
- <sup>37</sup> M. Calandra and S. Sorella, *Phys. Rev. B* **57**, 11446 (1998).
- <sup>38</sup> S. Sorella and L. Capriotti, *Phys. Rev. B* **61**, 2599 (2000).
- <sup>39</sup> This has been shown in Ref. 34, by proving that  $\langle \Phi | O | \Phi \rangle \geq 0$  for any wave function  $|\Phi\rangle$ .
- <sup>40</sup> G.J. Chen, R. Joynt, F.C. Zhang, and C. Gros, *Phys. Rev. B* **42**, 2662 (1990).
- <sup>41</sup> A.W. Sandvik, *Phys. Rev. B* **56**, 11678 (1997).
- <sup>42</sup> M. Calandra and S. Sorella, *Phys. Rev. B* **61**, 11894 (2000).
- <sup>43</sup> N. Furukawa and M. Imada, *J. Phys. Soc. Jpn.* **62**, 2557 (1993).
- <sup>44</sup> F.F. Assaad and M. Imada, *Phys. Rev. Lett.* **76**, 3176 (1996).
- <sup>45</sup> G. Kotliar, S. Murty, and M. Rozenberg, *Phys. Rev. Lett.* **89**, 046401 (2002).
- <sup>46</sup> D. Poilblanc, *Phys. Rev. B* **52**, 9201 (1995).